Searching for the Fractional Quantum Hall Effect in Graphite

Y. Kopelevich,[1] B. Raquet,[2,3] M. Goiran,[2,3] W. Escoffier,[2,3] R. R. da Silva,[1] J. C. Medina Pantoja,[1] I. A. Luk'yanchuk,[4] A. Sinchenko,[5,6] and P. Monceau[6]

[1]*Instituto de Física "Gleb Wataghin," Universidade Estadual de Campinas, UNICAMP 13083-970, Campinas, São Paulo, Brasil*
[2]*CNRS; UPR 3228 LNCMI; 143 Avenue de Rangueil, F-31400 Toulouse, France*
[3]*Université de Toulouse, UPS, INSA, LNCMI; F-31400 Toulouse, France*
[4]*Laboratoire de Physique de Matière Condensée, Université de Picardie Jules Verne, Amiens, 80039, France*
[5]*Moscow Engineering-Physics Institute, 115409, Moscow, Russia*
[6]*Institut Néel, CNRS, B.P. 166, 38042 Grenoble cedex 9, France*
(Received 12 March 2009; published 9 September 2009)

Measurements of basal plane longitudinal $\rho_b(B)$ and Hall $\rho_H(B)$ resistivities were performed on highly oriented pyrolytic graphite samples in a pulsed magnetic field up to $B = 50$ T applied perpendicular to graphene planes, and temperatures 1.5 K $\leq T \leq 4.2$ K. At $B > 30$ T and for all studied samples, we observed a sign change in $\rho_H(B)$ from electron- to holelike. For our best quality sample, the measurements revealed the enhancement in $\rho_b(B)$ for $B > 34$ T ($T = 1.8$ K), presumably associated with the field-driven charge density wave or Wigner crystallization transition. In addition, well-defined plateaus in $\rho_H(B)$ were detected in the ultraquantum limit revealing possible signatures of the fractional quantum Hall effect in graphite.

PACS numbers: 73.43.−f, 81.05.Uw

The behavior of matter in a very strong magnetic field (B) continuously attracts the interest of physicists working in various fields ranging from astrophysics [1,2] to semiconductors [3]. The field-induced Landau level quantization in (semi)conductors leads to a variety of spectacular phenomena such as, e.g., integer and fractional quantum Hall effects (IQHE and FQHE) in two-dimensional (2D) systems [3]. In three-dimensional (3D) samples, a strong enough field localizes the electron (hole) motion in the plane perpendicular to B, while the motion along B remains intact [4]; this can be viewed as the field-induced $3D \rightarrow 1D$ dimensional crossover. The reduced dimensionality in the electron system becomes pronounced for $B > B_{QL}$ (QL stands for quantum limit) that pulls all carriers into the lowest Landau level (LLL). In this limit, competing charge density wave (CDW) and superconducting correlations [5], or excitonic [6] instabilities driven by the field are expected. In addition, a field-induced Luttinger liquid state has been proposed [7]. Low carrier density 3D semimetals such as bismuth and graphite have been considered [5–7] as promising materials for the experimental observations of above phenomena. Very recently, 3D FQHE in both bismuth and graphite has been theoretically proposed [8,9], corroborating the experimental results obtained for bismuth [10]. In contrast to bismuth, graphite is extremely anisotropic material with weakly coupled graphene layers, in which exciting physics of one, two, or few layers can be revealed [11]. The present work reports the first experimental results showing that FQHE may occur in graphite, pointing out on its quasi-2D nature.

It has been known for a long time that magnetic field $B > 20$ T $> B_{QL} = 7$–8 T, applied along the hexagonal c axis, induces in graphite an anomalous high-resistance state (HRS) that can be detected using either basal-plane $\rho_b(B, T)$ or out-of-plane $\rho_c(B, T)$ resistivity measurements [12–18]. The boundaries that trace the HRS domain on the B-T plane [15,17] are in qualitative agreement with theoretical expectations [19] for the Landau-level-quantization-induced normal metal—charge density wave (CDW) as well as the reentrant CDW-normal metal transitions. However, while the CDW is predicted to occur in the direction of magnetic field [19], the experimental results [13,14] indicate the in-plane character of CDW, or formation of 2D Wigner crystal (WC) state(s) [20,21]. Supporting either CDW- or WC-based scenarios, the non-Ohmic electrical transport was measured in HRS [14,18]. Typically, for $T = 2$ K, the HRS emerges in the field interval 25 T $< B < 52$ T, and the HRS does not occur for $T > 10$ K [17].

So far, all the HRS studies [12–18] were performed on artificially grown Kish or natural single crystalline graphite samples. To the best of our knowledge, no measurements above 28 T [12] were performed for HOPG, and no Hall resistivity $\rho_H(B)$ measurements above 30 T [16] were made on any type of graphite.

Recent magnetoresistance [22,23] and scanning tunneling spectroscopy (STS) [24] experiments revealed the integer quantum Hall effect (IQHE) in graphite. The IQHE takes place only in strongly anisotropic (quasi-2D) HOPG samples with the room temperature out-of-plane/basal-plane resistivity ratio $\rho_c/\rho_b > 10^4$, and mosaicity $\leq 0.5°$ (FWHM obtained from x-ray rocking curves). Together with the high electron mobility $\mu \sim 10^6$ cm^2/V s [25], this makes HOPG a promising system for the FQHE occurrence.

In the present work, we studied magnetoresistance in
HOPG in pulsed magnetic field up to $B = 50$ T and
1.5 K $\leq T \leq 4.2$ K. The measurements were performed
in Ohmic regime with 300 ms for the total pulse length in
ac configuration, at LNCMPI (Toulouse, France). Addi-
tional measurements were made using Janis 9T-magnet
He-4 cryostat.

Commercially available HOPG samples ZYA and SPI-3
were measured. The sample parameters are: FWHM =
$0.4°$, $\rho_c/\rho_b = 4 \times 10^4$ ($\rho_b = 5$ $\mu\Omega$ cm and $\rho_c = 0.2$ Ω cm)
for ZYA, and FWHM = $3.5°$, $\rho_c/\rho_b = 3.8 \times 10^3$ ($\rho_b =$
40 $\mu\Omega$ cm and $\rho_c = 0.15$ Ω cm) for SPI-3 HOPG samples
(the resistivity data were obtained for $B = 0$ and $T =$
300 K). X-ray diffraction (Θ-2Θ) measurements revealed
a characteristic hexagonal graphite structure in the Bernal
($ABAB...$) stacking configuration, with no signature for
the rhombohedral phase and the following unit cell pa-
rameters: a = 2.48 Å and c = 6.71 Å.

Here, we report the results obtained on the ZYA sample
of dimensions $l \times w \times t = 2.5 \times 2.5 \times 0.5$ mm³. The
magnetic field was applied parallel to the hexagonal
c axis ($B\|c\|t$), and $\rho_b(B)$, $\rho_H(B)$ were recorded using
the van der Pauw method, sweeping the field between
-50 and $+50$ T.

From the data presented in Figs. 1(a) and 1(b), one
observes that $\rho_b(B)$ goes through the maximum at $B_{m1} =$
18 T, develops two local minima at $B_\alpha = 30$ T and $B_{\beta_1} =$
34 T, and passes through the second maximum at $B_{m2} \approx$
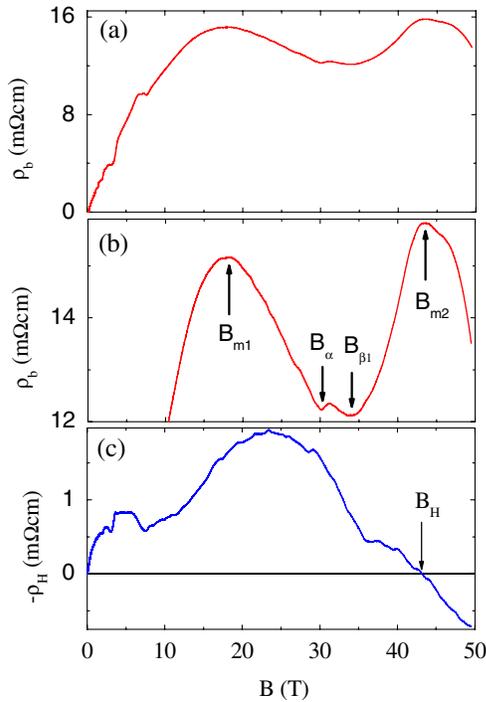

FIG. 1 (color online). (a) Basal-plane resistivity $\rho_b(B)$ mea-
sured up to $B = 50$ T at $T = 1.8$ K; (b) A detailed view of high-
field nonmonotonic behavior of $\rho_b(B)$ discussed in the text;
(c) Hall resistivity $\rho_H(B)$ demonstrating the sign change at
$B_H = 43$ T.

43 T. Thus, $\rho_b(B)$ represents all characteristic features
reported for Kish graphite [17], where, e.g., the resistivity
minima at $B_\alpha = 28$ T and $B_{\beta_1} = 33$ T, attributed to mul-
tiple field-induced CDW phases, were measured at $T =$
1.7 K.

The onset of HRS in Kish graphite is accompanied by a
rapid decrease of $\rho_H(B) \sim \sigma_H(B) = -e(n_e - n_h)/B$ [16],
where n_e and n_h are majority electron and hole carrier
densities, respectively. At low enough temperatures, $\rho_H(B)$
tends to zero as B approaches ~ 30 T, suggesting that
$\rho_H(B)$ may change its sign from "minus" to "plus" with
a further field increasing [16]. Our results [Fig. 1(c)] give
the experimental proof that the sign of $\rho_H(B)$ changes at
$B_H = 43$ T. The straightforward explanation of this effect
would be the carrier density imbalance change from $n_e >$
n_h ($B < B_H$) to $n_h > n_e$ ($B > B_H$). This provides us with a
new insight on the resistivity drop taking place at $B > B_{m2}$.
Namely, one assumes that decrease of both $\rho_b(B)$ and
$-\rho_H(B)$ at $B > B_{m1}$ originates from the hole density in-
crease [12], whereas the HRS is due to the field-induced
Wigner crystallization of electrons or CDW formation.
Then, nonmonotonic $\rho_b(B)$ can be simply understood us-
ing the equation for parallel resistors $\rho_b = \rho_{be}\rho_{bh}/(\rho_{be} +$
$\rho_{bh})$, [$\rho_{be}(B)$ and $\rho_{bh}(B)$ are electron and hole basal-plane
resistivities, respectively], without invoking any reentrant
transition in the electronic state (noting, $\rho_b \gg \rho_H$).

We also measured the similar sign reversal in $\rho_H(B)$ at
$B \sim 30$–35 T for two SPI-3 samples. However, due to a
poorer quality of those samples, neither negative magne-
toresistance nor HRS were detected. Instead, $\rho_b(B)$ satu-
rates for $B > 18$ T.

Next, we focus our attention on plateaulike and oscil-
latory features in $\rho_H(B)$ and $\rho_b(B)$, seen in Figs. 1–4 as a
fine structure.

In Fig. 2, we plotted $\Delta\rho_b(B)$ vs $1/B$ for $B < 5$ T, where
$\Delta\rho_b(B)$ is obtained after subtraction of the monotonic
background resistivity $\rho_b^{bg}(B)$: the data clearly demon-
strate that the fine structure is due to Shubnikov–de Haas
(SdH) oscillations. The obtained period of SdH oscillations
$\Delta(B^{-1}) = 0.208 \pm 0.004$ T^{-1} (the frequency $B_0 = 4.8 \pm$
0.1 T) corresponds to the extremal cross section of the
Fermi surface of the majority electrons [26].

The analysis of experimental results obtained for $B <$
B_{QL} [22,27] showed that electrons mainly contribute to the
measured $\rho_H(B)$, whereas the contribution from Dirac-like
majority holes is tiny [27]. Thus, the measured IQHE
staircase is consistent with either conventional massive
electrons with Berry's phase 0, or chiral massive electrons
having Berry's phase 2π, as in graphene bilayer [28,29].
We stress that IQHE staircases measured for HOPG
[22,27] and graphene bilayer samples [29] overlap when
plotted as a function of the filling factor $\nu = B_0/B$ [27],
testifying on the quasi-2D nature of HOPG. The inset in
Fig. 2 illustrates the QH plateau occurrence at $\nu = 1$ and
$\nu = 2$. In the same figure, we show $\rho_H(\nu)$ measured [22]
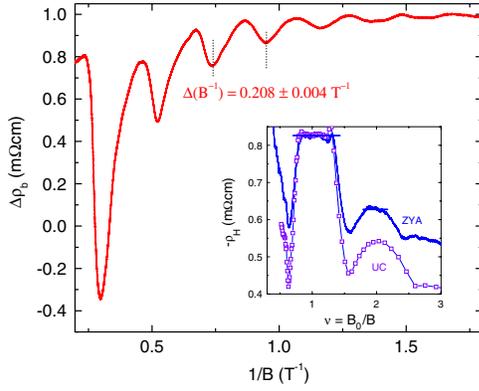for HOPG-UC (Union Carbide Co.) sample. It can be

FIG. 2 (color online). Shubnikov de Haas resistivity oscilla-
tions with the period $\Delta(B^{-1}) = 0.208 \pm 0.004$ T^{-1} correspond-
ing to the majority electrons; $\Delta\rho_b$ is obtained subtracting the
monotonic background resistivity $\rho_b^{bg}(B)$. The inset demon-
strates quantum Hall plateaus measured for HOPG-ZYA and
HOPG-UC [$\rho_H(B)/3.6$] samples; $\nu = B_0/B$ ($B_0 = 4.68$ T for
HOPG-UC, and $B_0 = 4.8 \pm 0.1$ T for HOPG-ZYA).

readily seen that the main IQHE plateau is centered at
$B = B_0$ for both ZYA and UC HOPG samples, demon-
strating the universality in the behavior of these strongly
anisotropic samples. The Hall resistivity $\rho_H(\nu = 1) =$
0.82 mΩ cm for ZYA HOPG was obtained from the mea-
sured Hall resistance $R_H(\nu = 1) = 16.5$ mΩ, assuming
the uniform current distribution through the sample thick-
ness $t = 0.5$ mm. Taking the distance between neigh-
boring graphene planes $d = c/2 = 3.355$ Å, one gets $N \approx$
1.5×10^6 independent graphene (bi)layers contributing to
the measured signal. This gives the Hall resistance per (bi)
layer $R_H^{\Box}(\nu = 1) = N \cdot R_H(\nu = 1) \approx 24.8$ kΩ,   that
practically coincides with the Klitzing fundamental Hall
resistance $h/e^2 \cong 25.8$ kΩ. However, because of the
strong sample anisotropy ($\rho_c/\rho_b = 4 \times 10^4$), the measur-
ing current can be concentrated within the effective
sample thickness $t_{\text{eff}} < t$ [30], implying that the actual
value of $R_H^{\Box}(\nu = 1)$ can be smaller. Taking the QH
plateau sequence $R_H^{\Box} = h/4\nu e^2$ as predicted (and mea-
sured) for graphene bilayer [28,29], and the measured dif-
ference $\Delta\rho_H(\nu) = \rho_H(\nu = 1) - \rho_H(\nu = 2) \approx 0.2$ mΩ cm
(Fig. 2, inset), one estimates the effective thickness of the
electron "layers" $l_{\text{eff}} \cong 6.2$ Å, responsible for IQHE.
Interestingly, the obtained value of l_{eff} agrees well with
the c axis lattice parameter $c = 6.71$ Å, resembling the
theoretical result for IQHE in bulk graphite [31]. Whether
this is an accidental coincidence or it has a deeper reason,
remains to be seen. The sample resistivity ratio $\rho_c/\rho_b =$
4×10^4 implies a very small tunneling amplitude in the c
axis direction $t_\perp \sim 3$–5 meV [11] $< \hbar\omega_c$ for $B > 1$–2 T,
allowing to consider independent QH states in each "bi-
layer," see also [32].

The data presented in Fig. 3 demonstrate that plateaus in
$\rho_H(B)$ also take place for $\nu \ll 1$. As Figs. 3(a)–3(c) exem-
plify, plateaus and quasiplateaus are centered quite accu-
rately (within the error bar for $B_0 = 4.8 \pm 0.1$ T) at
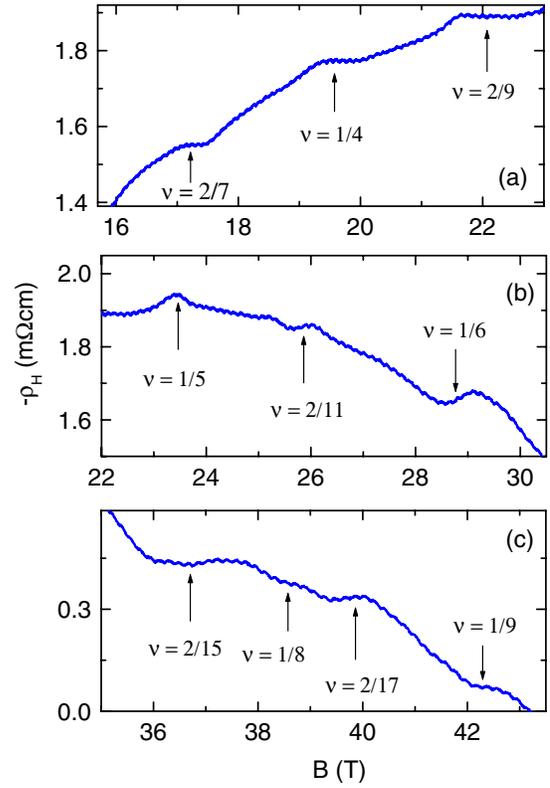

FIG. 3 (color online). Quantum Hall plateaus observed for
various fractional filling factors $\nu = B_0/B$ ($B_0 = 4.8 \pm 0.1$ T).

$\nu = 2/7$, $1/4$, $2/9$, $1/5$, $2/11$, $1/6$, $2/15$, $1/8$, $2/17$, $1/9$
[33]. It appears that all these numbers correspond to the
filling factors $\nu = 2/m$ ($m = 1, 2, 3, \ldots$) proposed by
Halperin [34] for the case of bound electron pairs, i.e.,
2e-charge bosons. In principle, the existence of $2e$ bosons
in the ultraquantum limit can be justified assuming the
electron pairing driven by the Landau level quantization
[5]. $\Delta\rho_H(B)$ steps between neighboring plateaus agree
with the FQHE scenario, as well. For instance, $\Delta\rho_H(B) \approx$
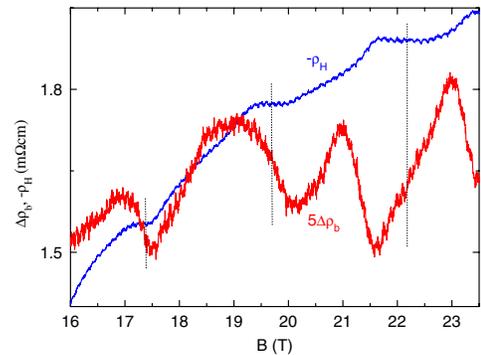0.22 mΩ cm measured between $\nu = 1/4$ and $\nu = 2/7$

FIG. 4 (color online). Plateaus in the Hall resistivity $\rho_H(B)$
correlate with the minima in $\Delta\rho_b$ (multiplied by factor 5 and
arbitrary shifted along the vertical axis); dotted lines mark
centers of QH plateaus.

[Fig. 3(a)] plateaus, coincides with the expected value $\Delta\rho_H(B) = (h/8e^2) \cdot c \approx 0.216$ mΩ cm.

It is worth noting that $l_{eff} \approx c = 6.71$ Å is much smaller than the magnetic length $l_B[\text{Å}] = (\hbar/eB)^{1/2} = 250/B^{1/2}[T^{1/2}]$ in the whole studied field range. Thus, recent 3D models for FQHE [8,9], probably relevant to bulk bismuth [10], do not apply to highly anisotropic graphite.

On the other hand, one may argue against the QHE in both bulk graphite and bismuth because $\rho_b(B)$ does not vanish in the plateau region, and $\rho_b(B) > \rho_H(B)$. However, small dips and not vanishing of the longitudinal resistivity $\rho_{xx}(B) > \rho_{xy}(B)$ were measured, e.g., for Bechgaard salt $(TMTSF)_2PF_6$ [35], $Bi_{2-x}Sn_xTe_3$ and $Sb_{2-x}Sn_xTe_3$ [36], η-Mo_4O_{11} [37] layered crystals, as well as for GaAs/AlGaAs 2DES [38,39], in both IQHE [35–37] and FQHE [38,39] regimes. In particular, in Ref. [39], FQH states resulting from the melted Wigner crystal were detected at very high global longitudinal resistance level of $R_{xx} \sim 1$ MΩ.

Figure 4 illustrates the correlation between QH plateaus and dips in $\Delta\rho_b(B)$ measured in the present work. Figure 4 also demonstrates that minima in $\Delta\rho_b(B)$ are somewhat shifted from the plateau centers which is the characteristic feature of QHE in bulk materials [36,37]. Thus, it is legitimate to treat the data obtained on graphite in a similar way. For $\nu > 2/7$, no correlation between dips in $\Delta\rho_b(B)$ and plateaulike features in $\rho_H(B)$ is found, and no plateaus corresponding to Halperin's $\nu = 2/m$ fractional filling factors can be unambiguously identified. Further studies should clarify this observation.

In summary, we report the results of basal-plane Hall resistivity $\rho_H(B)$ and longitudinal resistivity $\rho_b(B)$ measurements performed on HOPG samples up to $B = 50$ T. The sign change in the Hall resistivity from electron- to hole-type in ultraquantum limit is reported for graphite for the first time. For our best quality samples, FQHE associated with majority electrons is detected for filling factors $\nu \ll 1$, and ascribed to a quantum liquid of $2e$ bosons [34]. The obtained results provide evidence that strongly anisotropic graphite can be considered as a system of quasi-2D layers of the thickness $l_{eff} \approx c = 6.71$ Å that exhibit independent integer ($\nu \geq 1$) or fractional ($\nu < 1$) quantum Hall states.

[1] E. H. Lieb *et al.*, Phys. Rev. Lett. **69**, 749 (1992).
[2] M. Girart *et al.*, Science **324**, 1408 (2009).
[3] *Perspectives in Quantum Hall Effects: Novel Quantum Liquids in Low-Dimensional Semiconductor Structures*, edited by S. D. Sarma and A. Pinczuk (Wiley, New York, 1997).
[4] L. D. Landau and E. M. Lifshitz, *Quantum Mechanics* (Pergamon Press, Oxford, 1977), 3rd ed., Vol. 3.
[5] M. Rasolt and Z. Tesanovic, Rev. Mod. Phys. **64**, 709 (1992).
[6] A. A. Abrikosov, J. Low Temp. Phys. **2**, 37 (1970).
[7] C. Biagini *et al.*, Europhys. Lett. **55**, 383 (2001).
[8] F. J. Burnell *et al.*, **79**, 155310 (2009).
[9] M. Levin and M. P. A. Fisher, Phys. Rev. B **79**, 235315 (2009).
[10] K. Behnia *et al.*, Science **317**, 1729 (2007).
[11] Y. Kopelevich and P. Esquinazi, Adv. Mater. **19**, 4559 (2007).
[12] Y. Iye *et al.*, Phys. Rev. B **25**, 5478 (1982).
[13] G. Timp *et al.*, Phys. Rev. B **28**, 7393 (1983).
[14] Y. Iye and G. Dresselhaus, Phys. Rev. Lett. **54**, 1182 (1985).
[15] H. Ochimizu *et al.*, Phys. Rev. B **46**, 1986 (1992).
[16] S. Uji *et al.*, Physica B (Amsterdam) **246–247**, 299 (1998).
[17] H. Yaguchi and J. Singleton, Phys. Rev. Lett. **81**, 5193 (1998).
[18] H. Yaguchi *et al.*, J. Phys. Soc. Jpn. **68**, 181 (1999).
[19] D. Yoshioka and H. Fukuyama, J. Phys. Soc. Jpn. **50**, 725 (1981).
[20] H. Fukuyama *et al.*, Phys. Rev. B **19**, 5211 (1979).
[21] A. H. MacDonald and G. W. Bryant, Phys. Rev. Lett. **58**, 515 (1987).
[22] Y. Kopelevich *et al.*, Phys. Rev. Lett. **90**, 156402 (2003).
[23] K. S. Novoselov *et al.*, arXiv:cond-mat/0410631; Phys. Rev. B **72**, 201401 (2005).
[24] Y. Niimi *et al.*, Phys. Rev. Lett. **102**, 026803 (2009).
[25] I. L. Spain, in *Chemistry and Physics of Carbon*, edited by P. L. Walker (Dekker, New York, 1973), Vol. 8, p. 1.
[26] I. A. Luk'yanchuk and Y. Kopelevich, Phys. Rev. Lett. **93**, 166402 (2004).
[27] I. A. Luk'yanchuk and Y. Kopelevich, Phys. Rev. Lett. **97**, 256801 (2006).
[28] E. McCann and V. I. Fal'ko, Phys. Rev. Lett. **96**, 086805 (2006).
[29] K. S. Novoselov *et al.*, Nature Phys. **2**, 177 (2006).
[30] H. Kempa *et al.*, Phys. Rev. B **65**, 241101(R) (2002).
[31] B. A. Bernevig *et al.*, Phys. Rev. Lett. **99**, 146804 (2007).
[32] A. F. Garcia-Flores *et al.*, Phys. Rev. B **79**, 113105 (2009).
[33] Noting, the best agreement with the quoted filling factors one obtains assuming the increase of B_0 from 4.7 T ($\nu = 2/7$) to 4.9 T ($\nu = 1/9$) that may reflect the field-induced carrier density increase [12].
[34] B. I. Halperin, Helv. Phys. Acta **56**, 75 (1983).
[35] S. T. Hannahs *et al.*, Phys. Rev. Lett. **63**, 1988 (1989).
[36] M. Sasaki *et al.*, Physica B (Amsterdam) **298**, 510 (2001).
[37] M. Sasaki *et al.*, Solid State Commun. **109**, 357 (1999).
[38] L. W. Wong *et al.*, Phys. Rev. B **51**, 18033 (1995).
[39] W. Pan *et al.*, Phys. Rev. Lett. **88**, 176802 (2002).